Journal of Chromatography A 1642 (2021) 462030

Contents lists available at ScienceDirect

Journal of Chromatography A

journal homepage: www.elsevier.com/locate/chroma

Methodology of deconvolution of total solute retention on chemically modified stationary phases to structure specific contributions of bound compounds

Bohumil Dolenský*, Ameneh Tatar, Martin Havlík, Tereza Navrátilová, Jan Hajduch, Pavel Matějka

Department of Analytical Chemistry, University of Chemistry and Technology in Prague, Technická 5, 166 28 Praha, Czech Republic

ARTICLE INFO

Article history:
Received 8 January 2021
Revised 19 February 2021
Accepted 25 February 2021
Available online 3 March 2021

Keywords:
weak affinity chromatography
bound receptor
binding constant
retention factor
tweezer effect
retention mechanism

ABSTRACT

The total solute retention by a chemically modified stationary phase (CMSP) has been shown several times to be a potential tool for studying the binding abilities of the bound compound. In this article, we present a methodology for the deconvolution of the total retention into structure-specific contributions. Three complementary silica-based CMSPs were prepared: 1) non-modified silica, 2) silica modified by *syn*-bis-Tröger's base (a molecular tweezer) and 3) silica modified by *anti*-bis-Tröger's base (a non-tweezer molecule). These were characterized by elemental analysis and Raman spectroscopy, and used to assemble liquid chromatography (LC) columns. The total retention factors were estimated for electron-deficient nitro- and cyano-derivatives of benzene in both normal and reverse elution modes. The total retention factor was considered to be the sum of structure-specific retention factors, each related to the affinity (the binding constant) of a specific structure (the binding site), and its content in the modified silica, as defined for weak-affinity chromatography (WAC). The obtained structure-specific contributions are in line with the binding studies of ligands in solution. They reveal details of the retention mechanism, suggesting a more suitable attachment of ligands, and expose the shortcomings of evaluations based solely on the total retentions.

© 2021 Elsevier B.V. All rights reserved.

1. Introduction

A chemically modified stationary phase (CMSP), prepared by the covalent attachment of a ligand to a primal phase, not only shows a significant extension of chromatography performance, but also provides an opportunity to study the ligand itself, especially to assess intermolecular interactions between the ligand and solute molecules (so-called host–guest chemistry). Although these studies require the preparation of a CMSP and a liquid chromatography (LC) column, the method offers several significant advantages. Primarily, since most practical applications require ligands on solid surfaces (e.g., chemical sensors and smart surfaces), CMSP studies are more reliable for these applications than studies in solution, as there may be a fundamental difference between the behavior of ligands in solution and on a solid surface. In contrast to experiments in solution, CMSP studies enable an almost unlimited number of experiments without the consumption of the ligand, or the need for re-isolation. The consumption of solutes is negligible; in addition, they are re-isolated by the experiment. CMSP studies can be performed in various media, including those where the ligands or the solutes are poorly soluble. In addition, contemporary LC instruments enable the automation of those studies.

There are several impressive examples of a solution molecular receptor preserving its binding ability after covalent attachment to a stationary phase. The very first studies were introduced by Zimmerman et al. on molecular tweezer receptors [1,2] and receptors based on hydrogen bonds [3]. Linear correlations have been observed between the retention enthalpies of CMSPs and the binding enthalpies of related receptors in solution. On the other hand, on molecular tweezers of a different type, Klärner observed only similar trends between the binding ability in solution and the retention of corresponding CMSP, and used the linear solvation energy relationships (LSER) based on the Kamlet–Taft multiparameter scale to obtain a mechanistic insight on the retention process [4].

We are convinced that a direct correlation between the solution binding and the surface retention would be rare, as there are crucial factors that can fundamentally affect the functionality of a solution receptor after covalent bonding. In principle, any covalent attachment of a solution receptor to a surface results in

* Corresponding author.
E-mail address: Bohumil.Dolensky@vscht.cz (B. Dolenský).

https://doi.org/10.1016/j.chroma.2021.462030
0021-9673/© 2021 Elsevier B.V. All rights reserved.

changes of its molecular structure, accessibility to solute and solvent molecules, and its freedom of movement. In particular, the ideal attachment must: a) be in a part of the molecule where it would not negatively affect the binding ability due to its electron affinity or steric effect; b) provide proper orientation against the surface; c) have an adequate length and rigidity to ensure the proper accessibility of the binding site. In addition, the solid phase composition and surface morphology may play crucial roles. Failure to comply with any of these requirements may alter or completely eliminate the binding abilities observed in solutions. Unfortunately, there is no common method or evaluation strategy to study these particulars.

Traditionally, the functionality of CMSP is evaluated in bulk via the total retention, expressed by the single retention factor (k'), calculated from the retention time of the solute (t_R) and the void time (t_M) of the column (Eq. 1), or from the retention volume of the solute (V_R) and the void volume (V_M) of the column [5]. The volumes are calculated using the flow rate (FR) of the mobile phase (Eq. 2).

$$k' = (t_R - t_M)/t_M = (V_R - V_M)/V_M \quad (1)$$

$$V_M = FR \cdot t_M \quad (2)$$

However, it is common that the CMSP surface is not uniform, which results in several retention mechanisms, thus the net retention can be ambiguous. The same is true for interactions of an bound enzyme having various binding sites, for which it has been stated that the observed retention factor can be expressed as the sum of the retention factors of each individual mechanism of solute retention or distribution (Eq. 3, where x denotes a mechanism) [6].

$$k' = \sum_x k'_x \quad (3)$$

If a CMSP is considered as a multi-site receptor, then two border types can be identified based on the strength and selectivity of the interactions between the solute and the individual binding site (receptor) of the CMSP surface, usually quantified by the solute–receptor binding constant (K).

The first border type is typical for CMSP of affinity chromatography, having one strong and highly specific receptor–solute interaction. The primal phase is modified by a receptor, often having single-solute selectivity. Since the binding of the targeted solute is practically irreversible (K is typically from 10^5 to 10^{15} L/mol), the net retention is exclusively attributed to the receptor–solute interaction. The retention (binding) via surface areas without the receptor is negligible.

The second border type is typical for CMSP of reverse phase chromatography, having many weak and nonspecific interactions (K is typically ~1 L/mol). A solute interacts in various arrangements with a ligand, as well as with the unmodified surface areas. Although individual interactions are small and indistinguishable, many robust empirical methods have been developed for the classification, standardization, comparison, and quantification of specific intermolecular interactions; the prediction of solute retention based on its structure; the estimation of relationships between the solute structure and k'; and other purposes [5].

The remaining CMSPs, consisting of interactions of medium strength and selectivity, can be attributed to weak affinity chromatography (WAC) [7]. The binding constant of a bound receptor to a solute is typically 10^2 to 10^5 L/mol, which is a common value of artificial solution receptors. The k' of the solute is expressed as the product of the column constant C, which reflects column features such as the void fraction, porosity and density, the amount of available binding sites Q, and the binding constant of the bound receptor to a solute (Eq. 4). Under several commonly fulfilled considerations [8], k' can be expressed (Eq. 5) as the product of K and the molar concentration of binding sites in the column [Q]. By the combination of equations 1, 2, 4, and 5, the binding constant can be expressed (Eq. 6).

$$k' = C \cdot Q \cdot K \quad (4)$$

$$k' = K \cdot [Q] = K \cdot Q/(t_M \cdot FR) \quad (5)$$

$$K = k'/[Q] = FR \cdot (t_R - t_M)/Q \quad (6)$$

Recently, binding constants obtained from WAC have been shown to correlate with the constants from surface plasmon resonance (SPR) [9]. Great advances have been demonstrated in fragment screening using a monolithic column with only 3 μg of human serum albumin as a ligand [10]. In addition, both the binding constants and kinetics can be determined from WAC experiments [8].

In our contribution, based on the example of CMSPs modified by bis-Tröger's base (bisTB) derivatives [11,12], we demonstrate that a common comparison of the total retention-related CMSPs leads to shortcomings and ambiguities of the evaluation of the bound molecular receptor, as the consequence of non-ideal attachment and spurious retention via unmodified surface areas. We demonstrate that misinterpretation can be mostly eliminated, and more details on the receptor behavior can be revealed, when the degree of modification is thoroughly determined, and several retention mechanisms are considered for evaluation of the retention.

2. Experimental section

2.1. Chemicals and materials

Common solvents and reagents for synthesis, 1,2-, 1,3-, and 1,4-dicyanobenzene (*o*DCB, *m*DCB, and *p*DCB); 1,2,4,5-tetracyanobenzene (TCB); 1,2-, 1,3-, and 1,4-dinitrobenzene (*o*DNB, *m*DNB, and *p*DNB); 1,3,5-trinitrobenzene (TNB); and 1,3,5-tri-*t*-butylbenzene (TBB), were purchased from commercial providers (purity >98%) and used without further purification. Triethylamine (TEA) and dimethylformamide (DMF) of p.a. quality were used. HPLC-grade acetonitrile (ACN), *n*-heptane (HEP), and dichloromethane (DCM) and re-distilled water were used for chromatography. 3-Aminopropyl-functionalized silica Separon SGX NH_2, particle size ~7 μm, pore size 8 nm (Tessek Ltd.).

2.2. Nuclear Magnetic Resonance

Common NMR spectra were recorded at 22 °C on a Mercury Plus 300 NMR spectrometer (Varian) operated at 300 MHz for ^{1}H and 76 MHz for ^{13}C. The ^{1}H and ^{13}C chemical shifts are given in ppm using tetramethylsilane (TMS) as the internal standard (δ = 0 ppm); coupling constants are given in Hz.

The titration experiments followed by ^{1}H NMR were performed at 25.0 ± 0.1 °C in $CDCl_3$ (freshly re-distilled from Al_2O_3 and molecular sieves 3 Å), using TMS as the internal standard. Stock solutions were prepared by dissolving 4.6 mg of TCB in 22.4 mL of $CDCl_3$, 18.5 mg of *syn*-**1** in 5.7 mL of the TCB solution, and 18.5 mg of *anti*-**1** in 5.7 mL of the TCB solution. A series of 17 samples for each receptor (*syn*-**1** and *anti*-**1**) were prepared by mixing the stock solutions in different ratios using Hamilton syringes. The TCB concentration was constant, whereas the concentration of the receptor varied. The recorded spectra were processed and the chemical shift of TCB was used for determination of the binding constant K using the standard procedure [13].

2.3. Raman spectroscopy

NIR-excited Raman spectra were collected on an FT-Raman spectrometer (FT-NIR spectrometer EQUINOX 55, Raman module FRA 106/S, Nd:YAG laser, excitation wavelength 1064 nm, laser power ca. 150 mW, and Ge diode detector (Bruker Optics) cooled with liquid nitrogen). The scattered light was collected in back-scattering geometry. A total of 1024 scans were co-added to obtain an individual spectrum with a 2-cm^{-1} spectral resolution. More than 60 spectra were averaged, and spectral deviation records were calculated for each of CMSP samples analyzed to improve the signal/noise ratio and to ensure representativeness of the data. The spectra were acquired and processed using OPUS 5.5 software (Bruker Optics). Baseline-corrected band areas were calculated for semi-quantitative comparison. Baseline-corrected and subtracted spectra (using appropriate reference spectra) were used for detailed mutual comparison.

2.4. Preparation of dichlorides anti-**3** and syn-**3**

BisTB diastereomers *anti*-**1** and *syn*-**1** were prepared previously [14]. Diester *anti*-**1** (200 mg, 343 µmol) was treated with 2 M aq. NaOH in methanol at 75 °C overnight. The reaction mixture was neutralized by acetic acid dropwise. The precipitate was filtered off, washed with water and methanol, and dried in vacuo at 40 °C to obtain 165 mg (89%) of diacid *anti*-**2**. Analogously, diacid *syn*-**2** (172 mg, 90%) was prepared from diester *syn*-**1**.

Dichlorides *anti*-**3** and *syn*-**3** were prepared instantly before use. A corresponding diacid **2** (50 mg, 90 µmol) was treated with $SOCl_2$ (40 µL, 548 µmol) in toluene (5 mL) at 80 °C for 2 h. The resulting solution was evaporated in vacuo (co-evaporation with dry toluene) to dryness to give the corresponding chloride **3**.

2.5. Preparation of CMSPs and fabrication of LC columns

Freshly prepared chloride *anti*-**3** (or *syn*-**3**, or no chloride, 90 µmol) was dissolved in DMF (5 mL) and was added to a suspension of aminopropylated silica (1 g, 1.55 mmol of NH_2 groups) and TEA (40 µL, 287 µmol) in DMF (30 mL). The reaction mixture was stirred at 50 °C for 5 days. The silica was filtered off, washed with DMF, water, acetonitrile, and methanol, and dried in vacuo at 50 °C to give silica *anti*-SG-NH_2 (or *syn*-SG-NH_2, or SG-NH_2). The prepared silicas were characterized by Raman spectroscopy (vide infra) and elemental analysis.

Each silica was treated separately with acetyl chloride (0.12 mL, 1.7 mmol) and TEA (0.5 mL, 3.6 mmol) in acetonitrile (30 mL) at room temperature for 2 days. The obtained CMSP *anti*-SG (or *syn*-SG, or SG) was filtered off, washed with acetonitrile, water, and methanol, and dried in vacuo at 50 °C. The prepared CMSPs were characterized by Raman spectroscopy (vide infra) and elemental analysis.

Elaboration of the elemental analyses revealed the hydrogen and nitrogen content to be less reliable, since the values are rather small. In addition, the hydrogen content rather varied (particularly in SG-NH_2 and SG), which could be the consequence of the hygroscopicity of silica, as we observed in another of our research works. Hence, for all calculations we used the carbon content in the freshly dried samples (see Suppl. Mat.).

The prepared CMSPs were packed into LC columns (stainless steel, 80 × 4.0 mm) by the down fill technique as a methanol suspension under a pressure of 60 MPa. After all chromatography experiments, the columns were dried by a stream of dry gaseous nitrogen and the CMSPs were removed from the columns, dried in vacuo at 50 °C, and weighted. The amounts of CMSPs were 426 mg of SG, 450 mg of *anti*-SG and 491 mg of *syn*-SG.

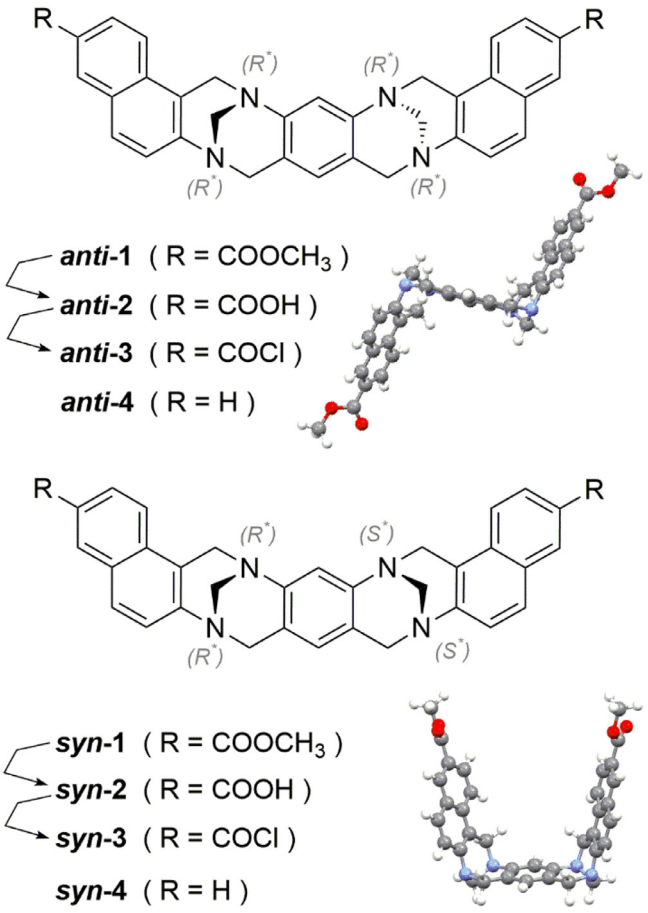


Chart 1. The molecular structures and models of studied bisTB diastereomers

2.6. High-performance liquid chromatography

The examinations of solutes were performed by means of isocratic elution at a flow rate of 1 mL/min (2A 250V SLO BLO piston pump, Cole-Parmer), using UV detection at 254 nm (785A, Perkin Elmer). The experiments were carried out at 20°C, with 20 μL injection volume. The solute concentration was 12.5 μg/mL, i.e., TBB 50.7 μmol/L, TCB 70.2 μmol/L, DCBs 97.6 μmol/L, TNB 58.7 μmol/L, and DNBs 74.4 μmol/L, in DCM for the normal phase mode (DCM-HEP 1:3 or 2:1, v/v), and in ACN/H_2O (1:1, v/v) for the reverse phase mode (0.5% v/v of ACN in water). The retention times were approximated at the peak apex of analysis of a single solute sample, since reading the values from an analysis of a solute mixture was complicated by peak overlaps. The retention time of TBB was used as the void time of the tested columns, since TBB was recommended and used in similar works [2,4].

3. Results and discussion

For our study, aimed at the elucidation of structure-specific contributions, we chose bisTB derivatives [11,12] in which a *syn* diastereomer represents the molecular tweezer receptor, whereas an *anti* diastereomer represents a non-tweezer-shaped molecule, entirely due to its stereostructure. Thus, the comparison of the binding affinity between the bisTB diastereomers can best demonstrate the tweezer effect (Chart 1). We chose *syn*-**1** and *anti*-**1** bisTB [14], which contain ester groups enabling their attachment to aminopropylated silica via the amide bond through corresponding acylchlorides.

3.1. Binding ability in solution

First, by comparison of the binding constants of bisTB **1** diastereomers, we confirmed that *syn*-**1** behaves as a molecular tweezer, contrary to *anti*-**1**. We determined the 1:1 binding constants (K) with 1,2,4,5-tetracyanobenzene (TCB) by NMR titration in $CDCl_3$. In comparison to the association constants of bisTB **4** [12,15], in which the naphthalene units bear no substituent, the four-times lower affinity of *syn*-**1** ($K^{syn\text{-}\mathbf{1}}$ = 25±1 L/mol) to TCB than that of *syn*-**4** ($K^{syn\text{-}\mathbf{4}}$ = 103±2 L/mol) can be attributed to the electron-withdrawing effect of the $COOCH_3$ group, which decreases the π-donor character of naphthalene, and consequently the ability to bind electron-deficient compounds. Although the magnitude of the association constants of the *anti* diastereomers are not fully reliable due to high relative uncertainty ($K^{anti\text{-}\mathbf{1}}$ = 3±1 L/mol, $K^{anti\text{-}\mathbf{4}}$ = 8±4 L/mol), the tweezer effects (TE = log $K^{tweezer}$ - log $K^{non\text{-}tweezer}$) of bisTB **1** and **4** are similar (TE = 0.9 and 1.1, respectively).

3.2. Preparation and characterization of modified silica

The required dichlorides, *anti*-**3** and *syn*-**3**, were prepared from corresponding diesters *anti*-**1** and *syn*-**1** via the routine two-step procedure (Scheme 1): diester **1** was hydrolyzed under alkaline conditions to corresponding carboxylic acid **2**, which was converted to chloride **3** via treatment with $SOCl_2$.

The reference blank CMSP was prepared in two steps. The treatment of commercial aminopropylated silica with DMF and TEA gave the starting silica (SG-NH_2). The following treatment with an acetylchloride excess gave the SG, in which all of the available NH_2 groups were converted into the AcNH groups.

The comparison of the carbon content in SG-NH_2 and SG revealed that there were 0.48 mmol/g of acetyl groups introduced; i.e., the starting silica SG-NH_2 contains 0.48 mmol/g of NH_2 groups available for acetylation. This is much less than stated by the manufacturer (1.5-2.2 mmol/g; 1.55 mmol/g by our elemental analysis), but in accordance with the usual degree of modification (0.3-0.5 mmol/g) [16]. Approximately 70% of the functional groups of silica are unavailable for modification.

The acetylation was also followed by Raman spectra. Although the spectral bands were weak, several pieces of evidence are unambiguous. The bands of NH_2 at 3315 cm^{-1} and C-N at 1064 cm^{-1} disappeared, whereas the bands related to the CH_3 group of introduced acetyl at 2940, 1442, and 1383 cm^{-1} appeared. We also observed the broad bands of amide I at 1663 and 1628 cm^{-1}, and the broad band of amide III at 1288 cm^{-1}. The broadness of the bands could be the consequence of a disorder caused by the variety of hydrogen bonds of the CO-NH groups with each other or with the groups on the silica surface. The bands of NH and amide II were not specifically resolved, probably due to their broadness.

The CMSP modified by *anti*-BisTB **1** was prepared in two steps. The treatment of SG-NH_2 with dichloride *anti*-**3** in DMF with TEA gave *anti*-SG-NH_2 silica, which was characterized by the elemental analysis and Raman spectra, and then treated with an excess of acetylchloride to convert the remaining NH_2 groups to the AcNH groups, to obtain the CMSP *anti*-SG.

The comparison of the carbon content in SG-NH_2, *anti*-SG-NH_2, and *anti*-SG revealed that 0.04 mmol/g (0.05 mmol/g based on the nitrogen content) of *anti*-bisTB (44% yield) and 0.45 mmol/g of acetyl groups were introduced. Since the sum of the introduced groups is approximately equal to the content of the acetyl groups in the reference SG, the dichloride *anti*-**3** is considered to be attached by a single carbonyl group and the attachment of *anti*-**3** does not protect surrounding NH_2 groups against the following acetylation. The second COCl group of *anti*-**3** was probably hydrolyzed to COOH during the work-up process.

The Raman spectra of the CMSPs confirmed the attachment of *anti*-bisTB, particularly by the bands at 3057, 2936, 2893, 1625, 1577, 1477, 1405, 1393, and 1375 cm^{-1}, as is evident from comparison with the spectrum of pure *anti*-bisTB **1** in solid. Broad bands at 1648 and 1292 cm^{-1} can be attributed to vibrational modes of amide groups. Unfortunately, no bands suggest the presence of the expected COOH group. Similarly to SG, the spectrum also shows the bands of the acetyl group.

The CMSP modified by *syn*-bisTB was prepared analogously to *anti*-SG using *syn*-**3** instead of *anti*-**3**, however, with a significantly different result. The carbon content in *syn*-SG-NH_2 revealed that 0.08 mmol/g (0.10 mmol/g based on the nitrogen content) of *syn*-bisTB was attached (89% yield). The attachment of *syn*-bisTB was also proved by the Raman spectra, and the twice-as-high content of bisTB on *syn*-SG-NH_2 than *anti*-SG-NH_2 was also confirmed by a detailed comparison of the Raman spectra (see Suppl. Mat.).

We suppose that the higher modification by *syn*-**3** than *anti*-**3** is a result of the higher reactivity of *syn*-**3** due to a cooperative effect, e.g., *syn*-**3** can be non-covalently bound to a surface aminopropyl group via the interaction of COCl (or COOH as a product of partial hydrolysis) with NH_2; thus, the second COCl group has a higher probability of acylating a nearby amine group. In addition, the binding of an aminopropyl group into the *syn*-**3** cavity could play a similar role.

More surprisingly, the elemental analyses of *syn*-SG revealed that only 0.26 mmol/g of acetyl groups were introduced. This means that the total modification of *syn*-SG is significantly lower than in the case of both SG and *anti*-SG (0.34 versus 0.48 and 0.49 mmol/g). This may be a consequence of the molecular shape of *syn*-**3**, which has the acyl groups on the same side of its molecule (Scheme 1); thus, a double attachment is more probable. The proposed double attachment would consume twice as many amine groups; thus, less of them can be subsequently acetylated.

The molecular geometry of *syn*-**3** optimized by semiempirical method PM3 revealed the spatial distance of the carbonyl groups to be 1.04 nm, and the angle formed by benzene and naphthalene moieties to be 105.5°. Since the angle can be from 80° to 114°, as found in various Tröger's base derivatives [17], the distance in *syn*-**3** can be expected to be from 0.07 to 1.27 nm.

By considering 0.48 mmol of NH_2 groups per g of silica, and the surface of aminopropylated silica to be approximately 500 m^2/g (stated by the manufacturer), it can be calculated that there is one NH_2 group per 1.73 nm^2 of the silica surface. Under considerations of idealized uniform hexagonal packing of circles, a straight surface, and perpendicular orientation of all aminopropyl groups, the average distance between the two NH_2 groups would be 1.41 nm. In contrast, we found the surface is 269 m^2/g [16], which gave the average spacing 1.04 nm.

It would seem that the possibility of the double attachment of *syn*-**3** is probable when the smaller surface is accepted, however, there are at least three reasons to expect the double attachment even for the larger surface. Firstly, the aminopropyl groups are not distributed uniformly, but mostly statistically [18]. The void areas decrease the surface for the aminopropyl groups and thus decrease both local and average spacing. Thus, in clustered areas, the spacing can be as short as the distance of the two silicon atoms, which is from 0.301 to 0.327 nm [19]. Secondly, the aminopropyl groups can be tilted to each other due to rotation around single bonds of the aminopropyl groups, or due to the local convexity of the silica surface. As the C-N distance in the all-*trans* configuration of $\underline{C}H_2$-CH_2-CH_2-$\underline{N}H_2$ is 0.382 nm (from the PM3 optimized molecular model), the tilting of both aminopropyl groups towards by 29° shortens the amine distance to 1.04 nm, 45° to 0.87 nm, and 90° to 0.65 nm. Thirdly, the second attachment could be provided by a salt bridge between NH_3^+ and CO_2^- as the consequence of a partial hydrolysis of the COCl group. That would enlarge the distance

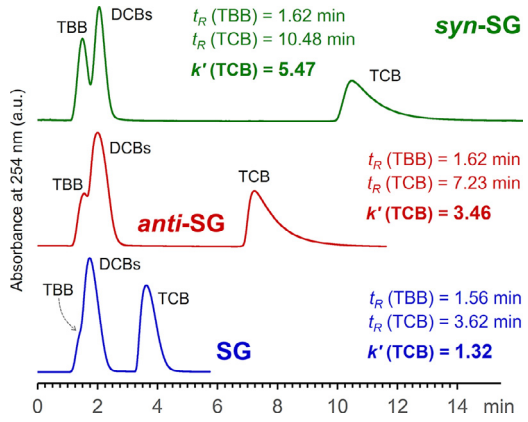


Fig. 1. Comparison of the CMSPs retention.
The chromatograms of LC separation of TBB, *o*DCB, *m*DCB, *p*DCB (the isomers are not resolved), and TCB mixture on *syn*-SG (top), *anti*-SG (middle) and SG (bottom) in the normal mode (HEP/DCM 1:2).

by at least 0.3 nm (the length of N-H and C-O bonds, and the ion–ion distance).

However, even if all *syn*-bisTB molecules were double attached, it is expected that 0.06 mmol/g of amine groups would still be acetylated. The lack of hindrance to acetylation observed in the case of *anti*-bisTB suggests that the amine groups are sequestered by the cavity of the attached *syn*-bisTB. We found no unambiguous evidence of the free aminopropyl groups in the Raman spectra. However, the integration of 1442 and 1288 cm^{-1} bands gave the contents of the acetyl groups on SG, *anti*-SG and *syn*-SG in the ratio of 45:36:18, which is similar to the ratio of 40:38:22 determined by elemental analyses.

Since we found no spectral evidence to support any specific molecular arrangements at the *syn*-SG surface, we considered the two border situations. The first possibility is that all *syn*-bisTB molecules are double attached and 0.06 mmol/g of aminopropyl chains are within their cavities, thus only 0.02 mmol/g of *syn*-bisTB (25%) would have empty cavities. The second possibility is that only 75% (0.06 mmol/g) of *syn*-bisTB molecules are double attached, and 0.08 mmol/g of cavities are occupied by aminopropyl chains, hence there would be no empty cavities to bind a solute. This means that only 0 to 25% of *syn*-bisTB molecules are capable of binding a solute via the molecular tweezer mechanism. Since the first possibility requires a small proximity of three aminopropyl chains, the second scenario is more probable.

Finally, we should notice that the differences between the Raman spectra of *anti*-SG and *syn*-SG were similar to those found between pure *anti*-**1** and *syn*-**1** [20]. Therefore, the isomerization between *anti* and *syn* configuration did not take place.

3.3. Evaluation of prepared CMSPs

To evaluate the binding abilities of bisTB derivatives on the silica surface, the prepared CMSPs were packed into the steel columns, and their retention abilities were studied via LC in both normal and reverse modes. The retentions were identical when the modes where switched back and forth. The retention factors were estimated for a series of solutes.

A direct comparison of the chromatograms from the CMSPs is in line with expectations (Fig. 1); however, there are several facts that call this comparison into question. The blank SG showed the weakest retention of the TCB (no arene–arene interactions, $k' = 1.32$), *anti*-SG to be stronger (arene–arene interactions, $k' = 3.46$) and *syn*-SG to be the strongest (arene–arene interactions and the tweezer effect, $k' = 5.47$). However, since the bisTB content

Table 1
Binding constants calculated from retention values of prepared chemically modified stationary phases (CMSPs), considering 25%, 10%, and 4% of free *syn*-bisTB cavities. The first half of the table rows is for the normal phase (HEP:DCM 3:1, 1:2 for TCB); the second is for the reverse mode (0.5% ACN in water).

			25% of cavities		*1% of cavities*		*4% of cavities*	
Solute	K^{Ac}	K^{Anti}	K^{Syn}	*TE*	K^{Syn}	*TE*	K^{Syn}	*TE*
*o*DNB	9.5	79	188	0.4	411	0.7	969	1.1
*m*DNB	5.4	54	95	0.2	197	0.6	452	0.9
*p*DNB	4.1	42	77	0.3	161	0.6	370	0.9
TNB	12.2	165	282	0.2	583	0.5	1333	0.9
*o*DCB	14.8	116	306	0.4	679	0.8	1610	1.1
*m*DCB	9.5	79	177	0.3	383	0.7	899	1.1
*p*DCB	9.6	79	164	0.3	350	0.6	817	1.0
TCB	10.1	198	474	0.4	1036	0.7	2440	1.1
*o*DNB	1.5	58	311	0.7	735	1.1	1793	1.5
*m*DNB	1.8	62	261	0.6	607	1.0	1471	1.4
*p*DNB	1.4	58	248	0.6	577	1.0	1399	1.4
TNB	0.9	74	253	0.5	577	0.9	1386	1.3
*o*DCB	1.0	40	133	0.5	303	0.9	729	1.3
*m*DCB	0.6	21	95	0.7	222	1.0	539	1.4
*p*DCB	0.5	22	105	0.7	247	1.1	602	1.4
TCB	0.5	56	247	0.6	576	1.0	1398	1.4

is twice as great on *syn*-SG as on *anti*-SG, the retention factors of *anti*-SG should be multiplied by two. This would lead to a surprising conclusion that *anti*-SG retains more than *syn*-SG, which is the opposite affinity of both bisTB **1** and **4** in solution (vide supra). At the same time, as there is the reasonable consideration that no more than 25% of *syn*-bisTB cavities are available for retention (vide supra), the retention factors for *syn*-SG should be multiplied at least by four. This returns the comparison to qualitative expectations. Unfortunately, a quantitative comparison would be obscure. For example, although the majority of the *syn*-bisTB cavities are disabled for binding, these molecules can still bind via their outer surface. In addition, there is also significant retention via the acetyl groups, as is evident from the SG column chromatogram (Fig. 1). Another deviation may originate from a different amount of CMSPs in the prepared columns. Obviously, the retention factors of both *anti*-SG and *syn*-SG should somehow be carefully corrected.

To assess the prepared CMSPs more accurately, we utilized the combination of the WAC relations between a retention factor and a binding constant (Eq. 5), and the consideration that the retention factor is the sum of the specific retention factors of several individual retention mechanisms (Eq. 3). As required by Equation 5, a 1:1 stoichiometric ratio of binding was assumed, although the reality can be different. All calculations are included in the Excel file of the Supp. Mat.

We consider the retention on SG exclusively as a result of the interaction with the acylated aminopropyl chains; thus, the retention factors can be expressed by Equation 7, and the binding constants can be calculated for each solute (Table 1). The K^{Ac} values are negligible in reverse mode separation (from 0.5 to 1.8 L/mol); however, they can be rather significant in the normal mode (from 4.1 to 14.8 L/mol). This is surprising, since stronger binding of hydrophobic molecules is expected for the reverse mode due to the hydrophobic effect. We contemplated that the acylated aminopropyl chains are hydrophobic, and thus protrude into the normal mode eluent, which enables the intercalation of solutes between the chains, although the chains are pressed onto the silica surface by the hydrophobic effect in the reverse mode eluent and thus minimize their effective surface for interaction.

$$k'_{SG} = \left[Q^{Ac}\right] \cdot K^{Ac} \tag{7}$$

In the case of *anti*-SG, we consider the total retention factor as the result of the retention via both *anti*-bisTB and the acylated aminopropyl chains, which is described by Equation 8. Using the

K^{Ac} values obtained from SG, the binding constants for bound *anti*-bisTB (K^{Anti}) can be calculated (Table 1). Contrary to K^{Ac}, the values of K^{Anti} from normal and reverse modes are in the same order. This may be a consequence of the larger size and higher rigidity of *anti*-bisTB molecules, rather than of the acylated aminopropyl chains. Thus, *anti*-bisTB molecules cannot be pressed onto the silica surface so tightly. In addition, the expected presence of the carboxylic acid functional group would increase the hydrophilicity of the bound *anti*-bisTB molecule.

In the case of *syn*-SG, we consider that the total retention factor is a result of retention via the acylated aminopropyl chains and the two forms of the bound *syn*-bisTB molecules. There is a fraction (n) of the *syn*-bisTB molecules with empty cavities, and a fraction (1-n) of molecules with the cavities filled by an aminopropyl chain. However, having no empty cavity does not necessarily mean no binding ability. Hence we consider that the retention via the later *syn*-bisTB molecules can be approximated by the retention via half the amount of *anti*-bisTB, since only the outer surface would be available for interactions in this case. We also consider that if an aminopropyl chain is unavailable for acylation, it is also unable to cause a retention. Thus, the total retention factor can be described by Equation 9.

$$k'_{anti-SG} = k'^{Ac} + k'^{Anti} = \left[Q^{Ac}\right] \cdot K^{Ac} + \left[Q^{Anti}\right] \cdot K^{Anti} \quad (8)$$

$$k'_{syn-SG} = \left[Q^{Ac}\right] \cdot K^{Ac} + (1-n) \cdot 0.5 \cdot \left[Q^{Syn}\right] \cdot K^{Anti} + n \cdot \left[Q^{Syn}\right] \cdot K^{Syn} \quad (9)$$

The calculated values show (Table 1) that if the presumed maximum proportion of empty cavities is considered (25%), then the K^{Syn} values are higher than the K^{Anti} values, as expected; however, TE on the CMSPs is less than half of the TE in the solution. The same TE as in the solution is obtained when 10% of the empty cavities are considered for the reverse mode and 4% are considered for the normal mode. The higher TE in the reverse mode can be a simple fact or the consequence of the lower blocking of the cavities via aminopropyl chains, as they probably lie tightly on the silica surface in the reverse mode (vide supra), and thus block fewer of the cavities.

Overall, both K^{Anti} and K^{Syn} on the CMSPs are more than one order higher than the corresponding binding constants of both bisTB **1** and **4** in the solution. This may be a consequence of different solvents, or a cooperative effect of the aminopropyl linker or functional groups of the nearest surface, or an overestimation of the presented evaluation method. Both values of K^{Anti} and K^{Syn} are the highest for the most electron-deficient solutes (TNB and TCB), as expected for arene–arene interactions, with the exception of nitrobenzenes in reverse mode, which suggests that different interactions are also presented in that case.

Finally, in all the cases, we observed that the *ortho* isomers of the solutes have higher affinity than the *meta* and *para* isomers, which is contrary to other molecular tweezers, which have the highest affinity to *para* isomers both in solution [21] and after a covalent attachment to a surface [4]. We believe the unique selectivity may be the essential property of bisTB derivatives, although the assistance of the nearest surface may also play a role.

4. Conclusions

We have shown that the ordinary comparison of CMSPs based on the total retention can give wrong or only accidentally correct conclusions. As a more faultless comparison, we have suggested a new methodology of deconvolution of the total retention in CMSPs into the structure-specific contributions of bound molecules. The basis of this is the determination of the ligand contents in a series of complementary CMSPs, and considering the total retention factor of each CMSP as the sum of the structure-specific retention factors.

As a proof of this concept, we have applied this methodology to three complementary CMSPs, which differ in the content and molecular structure of the ligands. We have obtained meaningful conclusions that were in line with known facts and general expectations. In addition, we have exposed reasonable details of the surface processes, which are not commonly accessible by the state-of-the-art method.

Although we are aware that several aspects of the presented methodology require further studies, we believe the methodology will enable the understanding of various chromatography issues at the molecular level. Moreover, the methodology enables the study of intermolecular interactions and the behavior of molecules on surfaces, which is difficult to achieve by means of contemporary analytical methods.

Supplementary materials

The Supplementary materials are available free of charge on the ScienceDirect website. Data from elemental analyses and chromatography experiments, including all the calculations (Excel file). Visualization of molecular size relations, NMR and MS characteristics of diacids **2**, and NMR titration experiments of *anti*-**1** and *syn*-**1**, and the processed Raman spectra of the prepared CMSPs (PDF file).

Declaration of Competing Interest

The authors declare that they have no known competing financial interests or personal relationships that could have appeared to influence the work reported in this paper.

Acknowledgement

This work was supported by the Czech Science Foundation (project no. 18-02597S), and by the Ministry of Education, Youth and Sports (program INTER-EXCELLENCE, project no. LTAUSA19065).

References

[1] a) C.-W. Chen, H.W. Whitlock, Molecular Tweezers: A Simple Model of Bifunctional Intercalation, J. Am. Chem. Soc. 100 (1978) 4921–4922, doi:10.1021/ja00483a063; b) S.C. Zimmerman, Molecular Tweezers: Synthetic Receptors for π-Sandwich Complexation of Aromatic Substrates, Bioorg. Chem. Front. 2 (1991) 33–71, doi:10.1007/978-3-642-76241-3_2; c) S.C. Zimmerman, Rigid molecular tweezers as hosts for the complexation of neutral guests, Top. Curr. Chem. 165 (1993) 71–102, doi:10.1007/BFb0111281; d) F.-G. Klärner, B. Kahlert, Molecular Tweezers and Clips as Synthetic Receptors. Molecular Recognition and Dynamics in Receptor–Substrate Complexes, Acc. Chem. Res. 36 (2003) 919–932, doi:10.1021/ar0200448; e) M. Harmata, Chiral Molecular Tweezers, Acc. Chem. Res. 37 (2004) 862–873, doi:10.1021/ar030164v; f) M. Hardouin-Lerouge, P. Hudhomme, M. Sallé, Molecular clips and tweezers hosting neutral guests, Chem. Soc. Rev. 40 (2011) 30–43, doi:10.1039/B915145C.

[2] a) S. C. Zimmerman, K. W. Saionz, Z. Zeng, Proc. Natl. Acad. Sci. USA, Chemically bonded stationary phases that use synthetic hosts containing aromatic binding clefts: HPLC analysis of nitro-substituted polycyclic aromatic hydrocarbons, 1993, 90, 1190-1193. https://doi.org/10.1073/pnas.90.4.1190;; b) S.C. Zimmerman, K.W. Saionz, Quantitative Host-Guest Complexation Studies Using Chemically Bonded Stationary Phases. A Comparison of HPLC and Solution Enthalpies, J. Am. Chem. Soc. 117 (1995) 1175–1176, doi:10.1021/ja00108a053; c) the usage of TBB as the void marker is recommended by W. H. Pirkle, C. J. Welch, J. Liq. Chromatogr., A convenient void volume marker for several chiral HPLC columns, 1991, 14, 1-8. https://doi.org/10.1080/01483919108049593..

[3] S.C. Zimmerman, W.S. Kwang, A Comparison of Enthalpies of Formation in Solution and Enthalpies for HPLC Retention for Hydrogen-Bonded Host—Guest Complexes, Angew. Chem. Int. Ed. 34 (1995) 2404–2406, doi:10.1002/anie.199524041.

[4] M. Kamieth, U. Burkert, P.S. Corbin, S.J. Dell, S.C. Zimmerman, F.-G. Klärner, Molecular Tweezers as Synthetic Receptors: Molecular Recognition of Electron-Deficient Aromatic Substrates by Chemically Bonded Stationary Phases, Eur. J. Org. Chem. (1999) 2741–2749 https://doi.org/10.1002/(SICI)1099-0690(199911)1999:11≤2741::AID-EJOC2741≥3.0.CO;2-K..

[5] a) T. Cserháti, K. Valkó, Chromatographic determination of molecular interactions: applications in biochemistry, chemistry, and biophysics, CRC Press, 1993; b) R. M. Smith (editor), Journal of Chromatography Library, 1995, 57, Elsevier Science B.V.; c) E. Lesellier, C. West, Description and comparison of chromatographic tests and chemometric methods for packed column classification, J. Chromatography A 1158 (2007) 329–360, doi:10.1016/j.chroma.2007.03.122; d) V. E. F. Heinzen, B. S. Junkes, C. A. Kuhnen, R. A. Yunes, Molecular Interactions, Molecular Interactions in Chromatographic Retention: A Tool for QSRR/QSPR/QSAR Studies, 2012, 25-48. https://doi.org/10.5772/37798..

[6] D.E. Martire, R.E. Boehm, Unified theory of retention and selectivity in liquid chromatography. 2. Reversed-phase liquid chromatography with chemically bonded phases, J. Phys. Chem. 87 (1983) 1045–1062, doi:10.1021/j100229a025.

[7] a) S. Ohlson, A. Lundblad, D. Zopf, Novel approach to affinity chromatography using “weak” monoclonal antibodies, Anal. Biochem. 169 (1988) 204–208, doi:10.1016/0003-2697(88)90275-8; b) D. Zopf, S. Ohlson, Nature, Weak-affinity chromatography 346 (1990) 87–88, doi:10.1038/346087a0; c) M. Wikström, S. Ohlson, J. Chrom. A, Computer simulation of weak affinity chromatography, 1992, 597, 83-92. https://doi.org/10.1016/0021-9673(92)80098-F;; d) M. Strandh, H.S. Andersson, S. Ohlson, Methods Mol. Biol., Affinity Chrom., Weak Affinity Chromatography 147 (2000) 7–23, doi:10.1007/978-1-60327-261-2_2.

[8] a) S. Ohlson, M.-D. Duong-Thi, Methods, Fragment screening for drug leads by weak affinity chromatography (WAC-MS) 146 (2018) 26–38, doi:10.1016/j.ymeth.2018.01.011; b) F. Tsopelas, A. Tsantili-Kakoulidou, Advances with weak affinity chromatography for fragment screening, Exp. Opinion Drug Discov. 14 (2019) 1125–1135, doi:10.1080/17460441.2019.1648425.

[9] M.-D. Duong-Thi, G. Bergström, C.-F. Mandenius, M. Bergström, T. Fex, S. Ohlson, Comparison of weak affinity chromatography and surface plasmon resonance in determining affinity of small molecules, Analytical Biochemistry 461 (2014) 57–59, doi:10.1016/j.ab.2014.05.023.

[10] L. Lecas, J. Randon, A. Berthod, V. Dugas, C. Demesmay, Monolith weak affinity chromatography for μg-protein-ligand interaction study, J. Pharm. Biomed. Anal. 166 (2019) 164–173, doi:10.1016/j.jpba.2019.01.012.

[11] a) C. Pardo, E. Sesmilo, E. Gutiérrez-Puebla, A. Monge, J. Elguero, A. Fruchier, New Chiral Molecular Tweezers with a Bis-Tröger's Base Skeleton, J. Org. Chem. 66 (2001) 1607–1611, doi:10.1021/jo0010882; b) M. Valík, B. Dolenský, H. Petříčková, V. Král, Coll. Czech Chem. Commun., Regio- and Stereoselectivity in Preparation of Benzene Bridged Bis- and Tris-Tröger's Bases, 2002, 67, 609-621. doi: 10.1135/cccc20020609..

[12] B. Dolenský, M. Havlík, V. Král, Oligo Tröger's bases—new molecular scaffolds, Chem. Soc. Rev. 41 (2012) 3839–3858, doi:10.1039/C2CS15307F.

[13] K. Hirose, A Practical Guide for the Determination of Binding Constants, J. Incl. Phenom. Macrocycl. Chem. 39 (2001) 193–209 , doi: 10.1023/A:1011117412693.

[14] M. Havlík, V. Parchaňský, P. Bouř, V. Král, B. Dolenský, Bridged bis-Tröger's base molecular tweezers as new cavitand family, Collect. Czech. Chem. Commun. 74 (2009) 1091–1099, doi:10.1135/cccc2009036.

[15] M. Havlík, V. Král, B. Dolenský, Overcoming Regioselectivity Issues Inherent in Bis-Tröger's Base Preparation, Org. Lett. 8 (2006) 4867–4870, doi:10.1021/ol061913m.

[16] D. Sýkora, K. Záruba, M. Butnariu, A. Tatar, H.M. Pham, M. Studenovský, P. Řezanka, V. Král, New multimodal stationary phases prepared by Ugi multicomponent approach, J. Sep. Sci. 43 (2020) 4178–4190, doi:10.1002/jssc.202000587.

[17] B. Dolenský, J. Elguero, V. Král, C. Pardo, M. Valík, Current Tröger's Base Chemistry, Adv. Heterocycl. Chem. 93 (2007) 1–56, doi:10.1016/S0065-2725(06)93001-3.

[18] a) N. Knorr, H. Brune, M. Epple, A. Hirstein, M.A. Schneider, K. Kern, Long-range adsorbate interactions mediated by a two-dimensional electron gas, Phys. Rev. B 65 (2002) 115420 1-5, doi:10.1103/PhysRevB.65.115420; b) T. Miyajima, S. Abry, W. Zhou, B. Albela, L. Bonneviot, Y. Oumi, T. Sanoc, H. Yoshitake, Estimation of spacing between 3-bromopropyl functions grafted on mesoporous silica surfaces by a substitution reaction using diamine probe molecules, J. Mater. Chem. 17 (2007) 3901–3909, doi:10.1039/B708084K; c) J. Nakazawa, B.J. Smith, T.D.P. Stack, Discrete Complexes Immobilized onto Click-SBA-15 Silica: Controllable Loadings and the Impact of Surface Coverage on Catalysis, J. Am. Chem. Soc. 134 (2012) 2750–2759, doi:10.1021/ja210400u.

[19] W.A. Baur, Silicon-oxygen bond lengths, bridging angles Si-O-Si and synthetic low tridymite, Acta Cryst B33 (1977) 2615–2619, doi:10.1107/S0567740877009029.

[20] B. Dolenský, V. Parchaňský, P. Matějka, M. Havlík, P. Bouř, V. Král, J. Mol. Struct., Determination of relative configuration of symmetrical bis-Tröger's base derivatives 996 (2011) 69–74, doi:10.1016/j.molstruc.2011.04.018.

[21] a) F.-G. Klärner, U. Burkert, M. Kamieth, R. Boese, J. Benet-Buchholz, Molecular Tweezers as Synthetic Receptors: Molecular Recognition of Electron-Deficient Aromatic and Aliphatic Substrates, Chem. Eur. J. 5 (1999) 1700–1707 https://doi.org/10.1002/(SICI)1521-3765(19990604)5:6≤1700::AID-CHEM1700≥3.0.CO;2-9; b) F.-G. Klärner, U. Burkert, M. Kamieth, R. Boese, Molecular tweezers as synthetic receptors: molecular recognition of neutral and cationic aromatic substrates. A comparison between the supramolecular structures in crystal and in solution, J. Phys. Org. Chem. 13 (2000) 604–611, doi:10.1002/1099-1395(200010)13:10⟨604::AID-POC271⟩3.0.CO;2-7.